J. Fluid Mech. (1973), *vol.* 58, *part* 3, *pp.* 517–537
Printed in Great Britain

On the stratified Taylor column

By NELSON G. HOGG

National Institute of Oceanography, Wormley, Godalming, Surrey†

(Received 22 June 1972 and in revised form 30 January 1973)

We analyse the effects of small, circularly symmetric topography on the slow flow of an inviscid, incompressible, diffusionless, horizontally uniform, baroclinic current and show that the vertical influence depends primarily on three parameters: a stratification measure S (the square of the ratio of buoyancy frequency times height scale to Coriolis parameter times length scale), a topographic parameter β (ratio of scaled topographic height multiplied by scaled bottom current to Rossby number ϵ) and the scaled upstream shear $u_0'(z)$ (the dimensional upstream shear divided by the ratio of the r.m.s. upstream flow speed to height scale).

Investigating a linear stratification model we find that the topographic effect is depth independent if $S \lesssim \epsilon$ and a Taylor column, as indicated by the appearance of closed streamlines above the bump, exists when $\beta > 2$. Moderate stratification ($S \sim 1$) causes the flow to be fully three-dimensional and the Taylor column to be a conical vortex whose height depends on β, S and $u_0'(z)$. The results are compared with Davies's (1971, 1972) experiments.

Our results tend to support the Taylor column theory of Jupiter's Great Red Spot but effects due to variations in the Coriolis parameter with latitude have been (unjustifiably) neglected. Using typical values for the earth's oceans we find that Taylor columns of significant height could be found there. Some pertinent observations from the ocean are discussed.

1. Introduction

Taylor (1917) and Proudman (1916) first discovered that the steady, infinitesmally slow flow of an inviscid, incompressible, homogeneous fluid in a rapidly rotating system is independent of the direction along the axis of rotation – a result now known as the Taylor–Proudman theorem. Consequently, such flow, between parallel planes perpendicular to the rotation axis and past isolated topography, must behave at all heights as it does near the topography. Provided that the topography is high enough, and it need only be infinitesmally high, the vertical velocity implied by the fluid having to rise over it may be inconsistent with the slow motion constraint and the fluid diverts to follow more closely the topographic bathymetric contours. If this happens a region of closed streamlines

† Present address: Department of Earth and Planetary Sciences, Massachusetts Institute of Technology.

whose pattern is depth independent may form above the obstacle. The region within these closed streamlines is known as a 'Taylor column' (Hide 1961). Taylor (1923) first observed the phenomenon in the laboratory. Amongst others, Hide & Ibbetson (1966), Hide, Ibbetson & Lighthill (1968), Vaziri & Boyer (1971) and Davies (1971, 1972) have continued the experimental investigation and extended the results qualitatively.

Let U be a typical speed, T a typical time scale for unsteady motion, L the horizontal scale of the topography, H the fluid depth, ν the coefficient of kinematic viscosity and $\frac{1}{2}f$ the angular speed of the rotating system about the vertical. For the Taylor–Proudman theorem to apply to such a flow the inherent assumptions imply that a time parameter $(fT)^{-1} \approx 0$ (steady motion), the Rossby number $\epsilon = U/fL \approx 0$ (slow motion) and that the Ekman number $E = \nu/fH^2 \approx 0$ (inviscid fluid). The incompressibility assumption is well approximated by many geophysical fluids, while the homogeneous constraint is the subject of this paper. Letting $\Delta\rho$ be a typical vertical density change over a depth H in a fluid of typical density ρ_0, this homogeneous requirement demands that a parameter

$$S = gH\Delta\rho/L^2f^2\rho_0 \approx 0.$$

To be specific we shall inquire into the effects of stratification when $S \lesssim 1$ and $1 \gg \epsilon \gg E^{\frac{1}{2}}$.

Within the range $1 \gg \epsilon \gg E^{\frac{1}{2}}$ Hide (1961) argued heuristically that a Taylor column could be forced in a homogeneous fluid by topography whose height exceeded the small value $\beta\epsilon H$, β being a number of order unity. Ingersoll (1969) showed rigorously that $\beta = 2$ for an obstacle of small circularly cylindrical shape and called the closed-streamline region, resulting when $\beta > 2$, an 'inertial' Taylor column (as opposed to the 'viscous' Taylor column problem of Jacobs (1964), who was interested in the range $1 \gg E^{\frac{1}{2}} \gg \epsilon$).

There has been some dispute over the effects of stratification on such an inertial Taylor column. By hypothesizing that the baroclinic component of flow should be much less than the barotropic for a topographic disturbance to be depth independent Stone & Baker (1968) and Ingersoll (1969) suggest the very restrictive criterion that $S \ll \epsilon \ll 1$. Hide (1971), however, in a general investigation of the steering influence of bottom topography derives a condition that can be rewritten as $S \ll 1$, $\epsilon \ll 1$, for the flow pattern to be two-dimensional, in agreement with an earlier study (Hide 1963) of flow over a two-dimensional ridge.

The object of this paper is to present a detailed analysis of the effects of stratification on the formation of inertial Taylor columns in a continuously stratified fluid. Consistently with Hide (1971), we find that the streamline pattern is two-dimensional when $S \ll 1$ and $\epsilon \ll 1$ (§§ 3 and 4). Even though the baroclinic component of the flow can be of the same magnitude as the barotropic when $S \sim \epsilon$ this z dependence is separable (equation (4.5) below), leaving a problem similar to Ingersoll's (1969). It is shown that a Taylor column will form above a small cylindrical obstacle if the obstacle height exceeds a critical value given by $h_c = 2HfLU^2/u_0^*(0)$, where

$$U = \left\{\int_0^H u_0^{*2}(z)\,dz/H\right\}^{\frac{1}{2}}$$

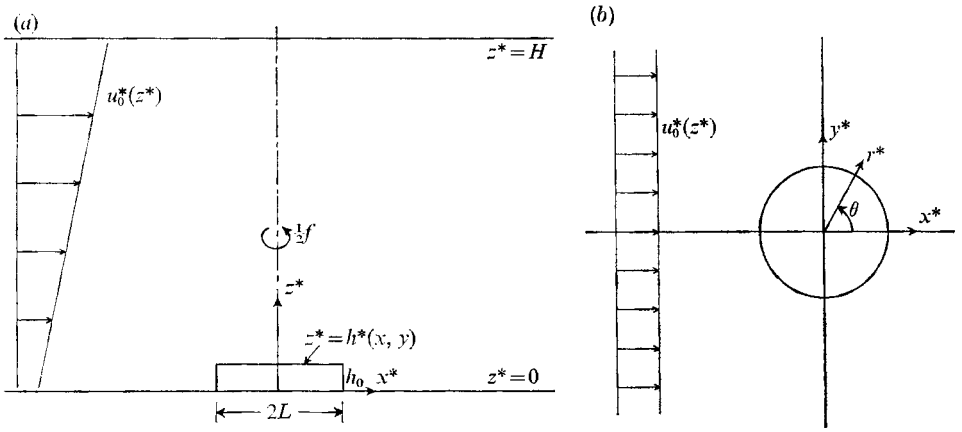

FIGURE 1. Notation: (*a*) side view; (*b*) top view.

is a velocity scale based on the upstream profile $u_0^*(z)$. Possible complications from the known instability (Eady 1949) of the undisturbed baroclinic flow are not considered.

The moderately stratified case, $S \sim 1$, is also studied (§5) and, as could be anticipated, it is found that the disturbance decays in the vertical and resembles a conical vortex. We show that the apex height of the vortex depends, primarily, on two parameters: the stratification measure S and a topographic number $\beta = h_0 f L u_0^*(0)/U^2$ (h_0 being the obstacle height). The result is compared with experiments by Davies (1971, 1972) (§6).

Some justification for the use of the inviscid limit is given in §7. In §8 we discuss the results in relation to Jupiter's Great Red Spot, and the earth's atmosphere and oceans.

2. Formulation

We wish to consider the influence of a small, localized bottom deformity on an incompressible, stratified fluid, flowing steadily between two otherwise horizontal plane surfaces, in a system rotating about a vertical axis with uniform angular velocity $\frac{1}{2}f$ (f is the Coriolis parameter). The independent variables of the fluid, density $\rho^*(\mathbf{x}^*)$, velocity $\mathbf{u}^*(\mathbf{x}^*) = (u^*(\mathbf{x}^*), v^*(\mathbf{x}^*), w^*(\mathbf{x}^*))$ and pressure $p^*(\mathbf{x}^*)$, are functions of a position vector $\mathbf{x}^* = (x^*, y^*, z^*)$ in a rotating Cartesian co-ordinate system. This co-ordinate system has unit vectors $\hat{\mathbf{i}}^*$, $\hat{\mathbf{j}}^*$ and $\hat{\mathbf{k}}^*$ with $\hat{\mathbf{k}}^*$ parallel to the rotation axis, $\hat{\mathbf{i}}^*$ directed downstream and the origin centred in the obstacle on the lower plane. The situation envisioned is illustrated by figure 1.

The obstacle geometry is given by the relation $z^* = h^*(x^*, y^*)$ while the upper surface is at $z^* = H$. We suppose that the bump is sufficiently small that if h_0 is a measure of its height then

$$\alpha = h_0/H \ll 1. \tag{2.1}$$

The typical horizontal dimension L of this topography is assumed to be a measure of the horizontal scale in the motion. The fluid depth H is taken to be the vertical length scale.

Far upstream from the obstacle the flow is uniform in the horizontal and $\mathbf{u}^*(\mathbf{x}^*) \to (u_0^*(z^*), 0, 0)$. The root-mean-square of $u_0^*(z^*)$ defines the velocity scale

$$U = \left\{\frac{1}{H}\int_0^H u_0^*(z^*)\,dz^*\right\}^{\frac{1}{2}}. \tag{2.2}$$

The fluid is statically stable with density variation $\rho^* = \rho_0 + \Delta\rho\rho_s(z^*/H)$ for a hypothetical rest state. Here ρ_0 is a constant reference density (that at $z^* = 0$ for instance), $\Delta\rho$ a measure of the density difference between bottom and surface ($\Delta\rho \ll \rho_0$) and $\rho_s(z^*/H)$ a (negative) normalized function giving the vertical variation.

The flow can be described qualitatively in terms of a number of non-dimensional parameters in addition to the obstacle height measure of (2.1). These are as follows:

$$\left.\begin{aligned} &\text{Rossby number} && \epsilon = U/fL,\\ &\text{Aspect ratio} && \delta = H/L,\\ &\text{Stratification measure} && S = (g\Delta\rho H/\rho_0 f^2L^2) = (N\delta/f)^2,\\ &\text{Ekman number} && E = \nu/fH^2,\\ &\text{Prandtl number} && \sigma = \nu/\kappa. \end{aligned}\right\} \tag{2.3}$$

In the above g is the acceleration due to gravity, $N = (g\Delta\rho/\rho_0 H)^{\frac{1}{2}}$ is the Brunt–Väisälä frequency and ν and κ are coefficients of kinematic viscosity and thermal diffusivity respectively. Our interests are primarily in small inertial effects on the flow in the range $\epsilon \sim \alpha \ll 1$. Viscous effects are for the most part neglected, a legitimate approximation if $\epsilon \gg E^{\frac{1}{2}}$ so that typical vertical velocities forced by advection past the topography are much greater than those developed by Ekman suction. Some complications involved in this inviscid limit are discussed in § 7. In this limit the Prandtl number is taken to be of order unity. Finally, the magnitude of the aspect ratio is restricted only to the extent that

$$\delta^2\epsilon^2 \ll 1,\dagger$$

so that the vertical momentum balance is hydrostatic at lowest order.

Using these parameters it is possible to non-dimensionalize the independent and dependent variables in the following manner:

$$\left.\begin{aligned} (x^*, y^*, z^*) &= L(x, y, \delta z),\\ (u^*, v^*, w^*) &= U(u, v, \delta w),\\ p^*(x^*) &= p_0 + p_s(z) + \rho_0 UfLp(\mathbf{x}),\\ \rho^*(\mathbf{x}^*) &= \rho_0 + \Delta\rho[\rho_s(z) + (\epsilon/S)\rho(\mathbf{x})], \end{aligned}\right\} \tag{2.4}$$

$p_0 + p_s(z)$ being the hydrostatic pressure produced by the basic stratification, that is

$$\partial p_s(z)/\partial z = -gH[\rho_0 + \Delta\rho\rho_s(z)].$$

The contributions $p(\mathbf{x})$ and $\rho(\mathbf{x})$ to the pressure and density arise from dynamic force balances.

† This can be formally verified *post hoc*, by noting that (2.10) below implies that the vertical velocity is of $O(U\delta\epsilon)$.

Substituting these expressions into the Navier–Stokes equations with the previously mentioned assumptions yields the following set of equations:

$$\left.\begin{aligned} \epsilon\mathbf{u}.\nabla u - v &= -p_x, \\ \epsilon\mathbf{u}.\nabla v + u &= -p_y, \\ 0 &= -p_z - \rho, \\ \epsilon\mathbf{u}.\nabla\rho + \rho_s'(z)\,Sw &= 0, \\ \nabla.\mathbf{u} &= 0. \end{aligned}\right\} \tag{2.5}$$

At the lowest order in ϵ the motion is hydrostatic and geostrophic. The Boussinesq approximation has been used to retain variable density effects only in the form of a buoyancy force in the vertical force balance.

We choose kinematic boundary conditions on the surface and bottom:

$$\left.\begin{aligned} w &= 0 \quad \text{on} \quad z = 1, \\ w &= \alpha\mathbf{u}.\nabla h \quad \text{on} \quad z = \alpha h(x,y), \end{aligned}\right\} \tag{2.6}$$

which specify that there be no normal component of velocity at the boundary. Far upstream the condition

$$\mathbf{u} \to (u_0(z), 0, 0) \quad \text{as} \quad \mathbf{x} \to \infty \tag{2.7}$$

is imposed.

From the set (2.5) it is possible to make two statements about the flow that hold for all ranges of stratification to be discussed. First we expand all the variables in a power series in the small Rossby number. For example

$$\mathbf{u}(\mathbf{x};\epsilon) = \sum_{n=0}^{\infty} \epsilon^n \mathbf{u}^n(\mathbf{x}) \tag{2.8}$$

is the expansion of the velocity vector. The lowest order horizontal momentum equations are

$$v^{(0)} = p_x^{(0)}, \quad u^{(0)} = -p_y^{(0)}, \tag{2.9}$$

which are equivalent to the definition of $p^{(0)}$ as a stream function. Substitution of (2.9) into the continuity equation shows that $w_z^{(0)} = 0$. As $w^{(0)} = 0$ on the upper boundary

$$w^{(0)} \equiv 0 \tag{2.10}$$

everywhere. The flow is approximately horizontal.

The second statement is derived from an elimination of $p^{(1)}$ from the $O(\epsilon)$ horizontal equations and use of the $O(\epsilon)$ continuity equation. We find that

$$(\mathbf{u}^{(0)}.\nabla_h = u^{(0)}\partial/\partial x + v^{(0)}\partial/\partial y) \qquad \mathbf{u}^{(0)}.\nabla_h \zeta^{(0)} = w_z^{(1)} \tag{2.11}$$

with $\zeta^{(0)} = v_x^{(0)} - u_y^{(0)} = \nabla_h^2 p^{(0)}$ being the vertical component of vorticity relative to the rotating frame. Equation (2.11) states that $O(1)$ changes in $\zeta^{(0)}$ and, consequently, in $v^{(0)}$, $u^{(0)}$ and the horizontal streamline pattern, occur if there are vertical variations in the small, $O(\epsilon)$, vertical velocity. For our situation this implies that the topography, although small, can have a significant effect on the horiziontal flow, if $\alpha \sim \epsilon$, through the vertical velocity imposed in (2.6).

Sections 3–5 will consider the manner in which this vorticity is distributed in the interior for varying degrees of stratification.

3. Very weak stratification: $S \ll \epsilon$

In the scaling equation (2.4) for $\rho^*(\mathbf{x}^*)$, $\epsilon\Delta\rho\rho(\mathbf{x})/S$ is the contribution to the density field needed to balance the Coriolis force at lowest order while $\rho_0 + \Delta\rho\rho_s(z)$ is the density present if there is no motion. As $\rho(\mathbf{x})$ is derived from the effects of motion on $\rho_s(z)$, $\epsilon\rho(\mathbf{x})/S \lesssim \rho_s(z)$. In this very weakly stratified regime $\epsilon/S \gg 1$, so that $\rho(\mathbf{x}) \sim S/\epsilon \ll 1$ and $\rho^{(0)} = 0$ because $\rho_s(z) \sim 1$.

From the hydrostatic balance, therefore,

$$p_z^{(0)} = 0. \tag{3.1}$$

Geostrophy at $O(1)$ implies, then, that

$$u_z^{(0)} = v_z^{(0)} = 0, \tag{3.2}$$

which, combined with the previously derived fact that $w_z^{(0)} = 0$, shows that the motion must be independent of z (the Taylor–Proudman theorem). At this degree of stratification the fluid behaves as it would if it were homogeneous.

This depth independence allows (2.11) to be integrated from bottom to surface yielding

$$(1-\alpha h)\,\mathbf{u}^{(0)}.\nabla\zeta^{(0)} = -(\alpha/\epsilon)\,\mathbf{u}^{(0)}.\nabla h. \tag{3.3}$$

If we neglect the small $O(\alpha)$ term in the depth integration then

$$\mathbf{u}^{(0)}.\nabla(\zeta^{(0)} + \beta h) = 0, \tag{3.4}$$

where

$$\beta = \alpha/\epsilon \tag{3.5}$$

is a topographic parameter. The quantity $\zeta^{(0)} + \beta h$ can be regarded as a potential vorticity which is conserved along streamlines. On streamlines which intersect topographic contours $\beta h > 0$ and $\zeta^{(0)}$ must decrease in order that potential vorticity be conserved. If $\zeta^{(0)}$ vanishes upstream, as in our case, negative relative vorticity is generated.

Using the fact that $\zeta^{(0)} \to 0$ upstream (3.4) can be integrated to show that

$$\nabla_h^2 p^{(0)} + \beta h = 0 \tag{3.6}$$

($\zeta^{(0)} = \nabla_h^2 p^{(0)}$ from geostrophy). Ingersoll (1969) has examined solutions to this equation for the special geometric case of a small, circular, cylindrical obstacle. He finds that there exists a critical value of β, β_c say, below which a Taylor column does not form, the Taylor column being defined by the appearance of closed streamlines. In the circular cylindrical case $\beta_c = 2$. For $\beta < \beta_c$ streamlines resemble those illustrated in figure 5(*c*) of § 5. For $\beta > \beta_c$ the pattern is qualitatively similar to figure 5(*a*). In general, when $\beta > \beta_c$ the Taylor column sits over the right side of the obstacle looking downstream.

Ingersoll (1969) investigated the long-term effects of viscosity on the fluid within the Taylor column noting that (3.6) is derived from imposed *upstream* conditions which do not necessarily apply to the region within a column. A discussion of this problem, with particular application to the moderately stratified regime, is given in § 7.

4. Weak stratification: $S \sim \epsilon$

The scaling relation for $\rho^*(\mathbf{x}^*)$ in (2.4) is now consistent with the density perturbation $\rho(\mathbf{x})$ being $O(1)$ and there is sufficient stratification that an $O(1)$ vertical shear can be supported by a horizontal density gradient in the thermal-wind manner (i.e. $u_z^{(0)} = \rho_y^{(0)}$, $v_z^{(0)} = -\rho_x^{(0)}$).

Because $w^{(0)} = 0$ the density conservation equation in (2.5) reduces to

$$\mathbf{u}^{(0)} . \nabla_h \rho^{(0)} = -\mathbf{u}^{(0)} . \nabla_h p_z^{(0)} = 0 \tag{4.1}$$

with the aid of the hydrostatic pressure equation. As $p^{(0)}$ is a stream function this equation can be integrated to show that

$$p_z^{(0)} = F(p^{(0)}), \tag{4.2}$$

$F(p^{(0)})$ being an, as yet, undetermined function of $p^{(0)}$. If we use the undisturbed upstream condition of (2.7), then

$$p^{(0)}(\mathbf{x}) \to -u_0(z)\, y \quad \text{as} \quad \mathbf{x} \to \infty, \tag{4.3}$$

$$p_z^{(0)}(\mathbf{x}) \to -u_0'(z)\, y = (u_0'(z)/u_0(z))\, p^{(0)} = F(p^{(0)}), \tag{4.4}$$

by integration of the geostrophic relations (2.9) for the undisturbed flow, setting $p^{(0)}(\mathbf{x}) = 0$ on $y = 0$ far upstream. We have, therefore, $p_z^{(0)}/p^{(0)} = u_0'/u_0$, an equation which is easily integrated with the important result that

$$p^{(0)}(x, y, z) = u_0(z)\, \psi(x, y). \tag{4.5}$$

In other words the z dependence in the stream function is separable and the streamline pattern is independent of depth. In particular if closed streamlines (i.e. a Taylor column) occur at one depth they must exist in a similar form (but with a different value, perhaps) at all other depths.

This conclusion can be slightly generalized so that it does not depend on upstream conditions. The local slope of a streamline in a horizontal plane is given by the ratio of $v^{(0)}$ to $u^{(0)}$, so that

$$\text{slope}\,(x, y, z) = v^{(0)}/u^{(0)} = -p_y^{(0)}/p_x^{(0)}. \tag{4.6}$$

If we differentiate (4.6) with respect to z we determine the manner in which the streamline slope depends on depth. This is

$$\begin{aligned} \frac{\partial}{\partial z}\,\text{slope}\,(x, y, z) &= -\frac{p_{yz}^{(0)}}{p_x^{(0)}} + \frac{p_y^{(0)} p_{xz}^{(0)}}{(p_x^{(0)})^2} \\ &= F'(p^{(0)}) \left(\frac{p_x^{(0)} p_y^{(0)} - p_y^{(0)} p_x^{(0)}}{(p_x^{(0)})^2} \right), \\ &= 0. \end{aligned} \tag{4.7}$$

As the horizontal streamline slope is depth independent the streamline shape, found from an integration of the slope, must be independent of depth as well.

The physical reason for this behaviour is the following. Suppose we consider the fluid to be composed of a large number of homogeneous layers each with a different density such that density increases with depth. This 'multi-layer' analogy is illustrated in figure 2. The motion within each layer will be depth

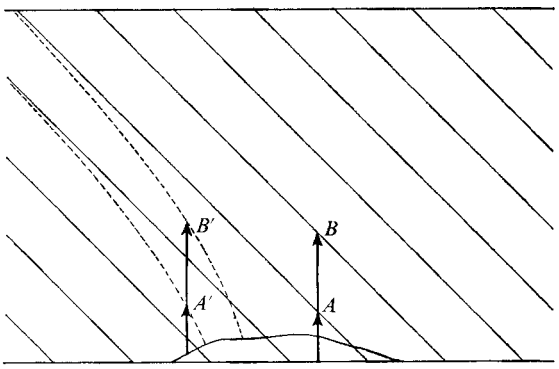

FIGURE 2. A multi-layer analogy of the density field for the weak stratification problem ($S \sim \epsilon$). We are looking downstream. The solid diagonal lines are the interfaces between layers far upstream from the obstacle. The dashed lines give the displaced positions of two interfaces at some point near the obstacle. A and B denote vertical vortex lines extending from bottom to top of their respective layers far upstream. A' and B' are the positions to which they have been carried by flow along streamlines.

independent according to § 3 and we can consider the concept of vorticity in terms of small vertical vortex lines extending from each layer bottom to its top (two such vortex lines are denoted by the letters A and B in figure 2). When such vortex lines are carried over topography they are compressed and this compression gives rise to negative relative vorticity.

Consider, now, the effect of topography on vortex line A in figure 2. As the motion carries it into contact with the bump, a slight compression is felt which produces $O(1)$ vorticity and a displacement to A' at some point in its travel past the bump. Geostrophy and continuity force the motion to be nearly horizontal.

Note, now, the effect of this distortion of the upper interface on vortex line B. The scaling relation of (2.4) for $\rho^*(\mathbf{x}^*)$ implies that, in order for the flow to have significant shear, the isopycnals (i.e. interfaces) must have an $O(1)$ slope in our stretched geometry. If vortex line B does not move in almost the same manner as A to position B' it will, therefore, suffer an $O(1)$ compression or extension which is incompatible with there being only $O(1)$ vorticity present and with the fact that $w^{(0)} = 0$.

Hide (1971) has derived a similar result using a scaling argument. In his terms, when a parameter $\sigma \equiv S^{-1} \gg 1$ the fluid at all depths is strongly 'steered' by topography.

The z dependence is separated by substitutions of the form

$$\mathbf{u}^{(0)}(x, y, z) = u_0(z)\,\mathbf{u}'(x, y), \tag{4.8}$$

so that the vorticity equation becomes

$$u_0^2(z)\,\mathbf{u}' \cdot \nabla\rho' = w_z^{(1)}. \tag{4.9}$$

Integrating from bottom to top as in § 3 and neglecting quantities of $O(\alpha)$ we find, as in (3.4), that

$$\mathbf{u}' \cdot \nabla(\zeta' + \beta h) = 0, \tag{4.10}$$

provided that the topographic parameter is redefined to be

$$\beta = (\alpha/\epsilon)\, u_0(0). \tag{4.11}$$

The dimensionless ratio $u_0(0) = u_0^*(0)/U$ enters through the bottom boundary condition and accounts for the fact that it is the bottom flow that actually senses the bump.

In a similar manner to Ingersoll's (1969) problem of § 3 we can integrate (4.10) to find a potential vorticity relation analogous to (3.6) and the critical value of β for the Taylor column formation. As before, $\beta_c = 2$ in the particular case of a small right circular cylinder.

We must emphasize that these conclusions, as stated, apply only to *steady* flow. It has been shown that baroclinic flows may be unstable to infinitesimal disturbances provided that S is less than a critical value of order unity (Eady 1949). No account of this effect has been made but the problem does not arise if the flow upstream is barotropic; the constraint of (4.5) forces it to remain barotropic in the presence of the bump.

5. Moderate stratification: $S \sim 1$

At this level of stratification the small isopycnal tilt $O(\epsilon/S)$ provides horizontal density gradients sufficient to balance the $O(1)$ vertical velocity gradient. With reference to the multi-layer analogy of § 4 this means that the vertical distortion of an interface by horizontal motions near the bump is $O(\epsilon/S) \ll 1$ consistent with the mechanism of $O(1)$ vorticity generation in each layer. Some of the compressing effect of the bump is taken up in a lower layer through the generation of relative vorticity, so that the one above sees a reduced effect. In this way the bump influence decays in the vertical – the form of this decay is the main subject of this section.

In order to simplify the mathematical analysis we further simplify the model to consider only a linear upstream velocity profile and undisturbed density gradient. Thus

$$u_0(z) = a + bz, \quad a^2 + ab + \tfrac{1}{3}b^2 = 1 \quad (a > -b,\, a > 0) \tag{5.1}$$

and

$$\rho_s(z) = -z, \tag{5.2}$$

where a and b are constants with the quadratic restriction in (5.1) being the non-dimensional version of (2.2). We further specify that $a > -b$, so that $u_0(z) > 0$. A flow reversal with depth gives rise to the possibility of a stationary wave pattern (essentially the short 'neutral waves' of the Eady (1949) baroclinic instability theory). This effect will not be discussed; nor will unstable waves themselves, but we note that the latter will have the positive phase speeds and so could not be directly excited by the obstacle.

From the density equation (2.5) we are able to compute the stretching term in the vorticity equation to be

$$\begin{aligned} w_z^{(1)} &= \frac{1}{S}\frac{\partial}{\partial z}(\mathbf{u}^{(0)} . \nabla_h \rho^{(0)}) \\ &= \mathbf{u}^{(0)} . \nabla_h (\rho_z^{(0)}/S), \end{aligned} \tag{5.3}$$

as $\mathbf{u}_z^{(0)}.\nabla\rho^{(0)} = 0$ from geostrophy and the hydrostatic pressure balance. Equation (2.11) becomes

$$\mathbf{u}^{(0)}.\nabla_h(\zeta^{(0)} - \rho_z^{(0)}/S) = 0. \tag{5.4}$$

$\zeta^{(0)} - \rho_z^{(0)}/S$ is a potential vorticity analogous to (3.6) and is conserved along streamlines. The term $-\rho_z^{(0)}/S$ measures the stretching effect of the separation between isopycnals in much the same way that βh did for the total fluid depth when the flow pattern was depth independent.

Using the $O(1)$ momentum equations we write the potential vorticity in terms of $p^{(0)}$, the pressure stream function. Equation (5.4) integrates to show that the potential vorticity is a function of $p^{(0)}$ which vanishes upstream. Therefore

$$\nabla_n^2 p^{(0)} + p_{zz}^{(0)}/S = 0, \tag{5.5}$$

valid everywhere except, possibly, within closed streamlines.

Boundary conditions (2.6) on the upper and lower surfaces can also be derived in terms of $p^{(0)}$. We have

$$0 = w^{(1)} = (\epsilon/S)\,\mathbf{u}^{(0)}.\nabla_h\rho^{(0)} \quad \text{on} \quad z = 1, \tag{5.6}$$

which integrates along streamlines to give

$$u_0(1)\,p_z^{(0)} - u_0'(1)\,p^{(0)} = 0 \quad \text{on} \quad z = 1. \tag{5.7}$$

The bottom condition is found from (2.6) by expanding $w^{(1)} = (\alpha/\epsilon)\,\mathbf{u}^{(0)}.\nabla_h\, h$ at $z = \alpha h(x, h)$ in a Taylor series about $z = 0$, and this gives

$$u_0(0)\,p_z^{(0)} - u_0'(0)\,p^{(0)} = -\beta S h \quad \text{on} \quad z = 0 \tag{5.8}$$

to lowest order.

We proceed to find a solution to the elliptic boundary-value problem posed by (5.5), (5.7) and (5.8) and the upstream condition given earlier in (4.3). To begin with, the geometry is chosen to be that of the small right circular cylinder for which it is convenient to work in the polar co-ordinates (r, θ, z) defined in figure 1. Therefore

$$h(r,\theta) = h(r)\begin{cases} = 1, & r < 1, \quad 0 \leqslant \theta \leqslant 2\pi, \\ = 0, & r > 1, \quad 0 \leqslant \theta \leqslant 2\pi, \end{cases} \tag{5.9}$$

is our chosen obstacle shape.

With this formulation it is a simple matter to obtain solutions in the two regions of (5.9) by the separation-of-variables method and then match them at $r = 1$. Vertical eigenfunctions $u_n(z)$ arise and are given by

$$u_n(z) = \frac{ak_n\cos k_n z + b\sin k_n z}{\displaystyle\int_0^1 (ak_n\cos k_n z' + b\sin k_n z')^2\,dz'} \qquad (n = 1, 2, \ldots), \tag{5.10}$$

with eigenvalues k_n, which are solutions to

$$\tan k_n = \frac{k_n}{1 + tk_n^2}, \quad t = \frac{a}{b}\left(\frac{a}{b} + 1\right) > 0. \tag{5.11}$$

So defined, the set $\{u_0(z), u_n(z)\}$ is orthogonal. The restriction that $t > 0$ arises from the assumption that the flow is unidirectional.

We find that

$$p^{(0)}(r,\theta,z) = -u_0(z)\, r\sin\theta - \tfrac{1}{2}\beta u_0(z)\ln r - S^{\frac{1}{2}}\beta \sum_{n=1}^{\infty} I_1(l_n)K_0(l_n r)\, u_n(z) \quad (r>1); \tag{5.12a}$$

$$p^{(0)}(r,\theta,z) = -u_0(z)\, r\sin\theta + \tfrac{1}{4}\beta(1-r^2)\, u_0(z) + S^{\frac{1}{2}}\beta \sum_{n=1}^{\infty} \left\{\frac{1}{l_n} - K_1(l_n)\, I_0(l_n r)\right\} u_n(z) \quad (r<1), \tag{5.12b}$$

having set $l_n = k_n/S^{\frac{1}{2}}$ for convenience. The functions $I_n(z)$ and $K_n(z)$ are modified Bessel functions of z. In the limit $S \to 0$ the series terms vanish from (5.12) and the solution found by Ingersoll (1969) to the homogeneous problem remains.

We have been primarily interested in the vertical influence of the obstacle as measured by the existence of closed streamlines in the flow field. Extrema in (5.12) for $p_r^{(0)}$, the azimuthal velocity, occur at the obstacle's lateral extremes. For there to be stagnation with no flow reversal at a given height the particular extremum is at $r = 1, \theta = -\frac{1}{2}\pi$ ($\beta > 0$) and, in order that a Taylor column appears at this level, the topographic parameter must exceed the critical value

$$\beta = \left\{\frac{1}{2} - \sum_{n=1}^{\infty} S^{\frac{1}{2}} l_n I_1(l_n)\, K_1(l_n)\, \frac{u_n(z)}{u_0(z)}\right\}^{-1} \tag{5.13}$$

found by setting $p_\theta^{(0)} = p_r^{(0)} = 0$ at $\theta = -\frac{1}{2}\pi$, $r = 1$.

The series term in β converges very slowly. If the S_N is the Nth term it can be shown that

$$u_0(z)\, S_N \to \frac{S^{\frac{1}{2}}}{aN\pi}\cos N\pi z + \frac{S^{\frac{1}{2}}}{(aN\pi)^{\frac{1}{2}}}\left(b - \frac{az}{r}\right)\sin N\pi z + O((N\pi)^{-3}). \tag{5.14}$$

By rewriting (5.13) in the form

$$\beta = \left\{\frac{1}{2} - \sum_{n=1}^{\infty} \frac{S^{\frac{1}{2}}}{u_0(z)}\left[l_n I_1(l_n)\, K_1(l_n)\, u_n(z) - \frac{\cos n\pi z}{an\pi}\right] - \sum_{n=1}^{\infty} \frac{S^{\frac{1}{2}}\cos n\pi z}{u_0(z)\, an\pi}\right\}^{-1}, \tag{5.15}$$

the first summation converges as $(n\pi)^{-2}$ while the second is evaluated exactly as (Gradshteyn & Ryzhik 1965, p. 38)

$$\sum_{n=1}^{\infty} \frac{\cos n\pi z}{u_0(z)\, n\pi} = -\frac{\ln[2(1-\cos\pi z)]}{2\pi u_0(z)}. \tag{5.16}$$

Using the altered expansion of (5.15) we computed the necessary β for a column to penetrate to a height z for a given stratification S and upstream shear $u_0'(z) = b$. The result is presented in figure 3 as contours of constant β. From an inspection of these curves several facts emerge. In the limit of small S, $\beta \to 2$ (see also figure 4) as we expect from the weak stratification section, but a weakly stratified column with $\beta = 2$ has a height of about $\frac{1}{3}$ if the stratification is non-zero. Note that the curves for $\beta > 2$ drop rapidly from $z = 1$ as S increases, and then flatten out at higher S to approach an almost constant level of about $z = \frac{1}{3}$. Apparently the volume of the column is constrained in some way and, although the stratification wishes to concentrate the disturbance near the bottom, the Coriolis forces work to limit its horizontal dimensions. We return to this observation in commenting upon Davies's (1971, 1972) experiments in the next section.

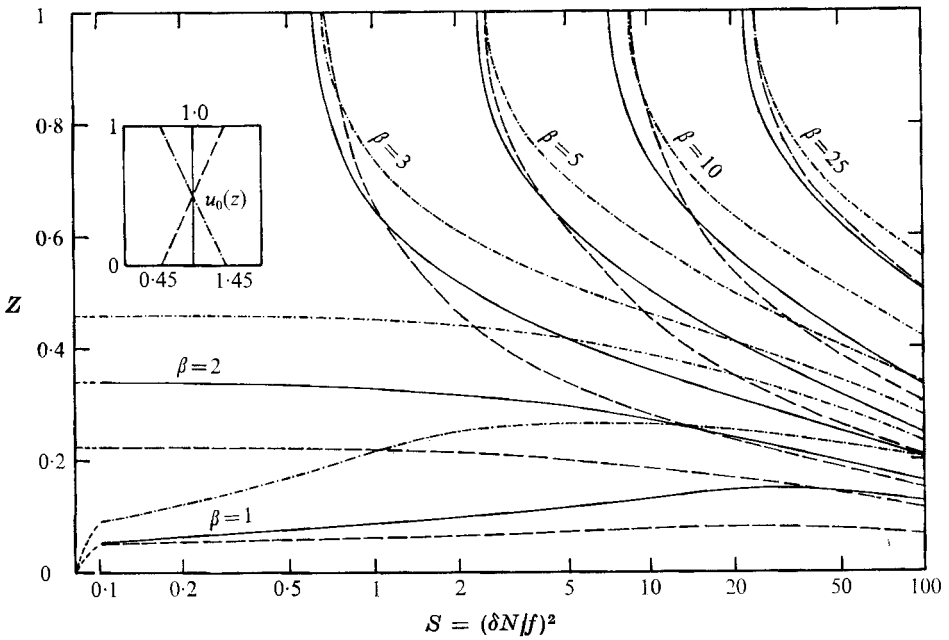

FIGURE 3. Graph of the penetration height versus S of a 'Taylor cone' forced over a circularly cylindrical bump for various β and $u_0'(z)$.

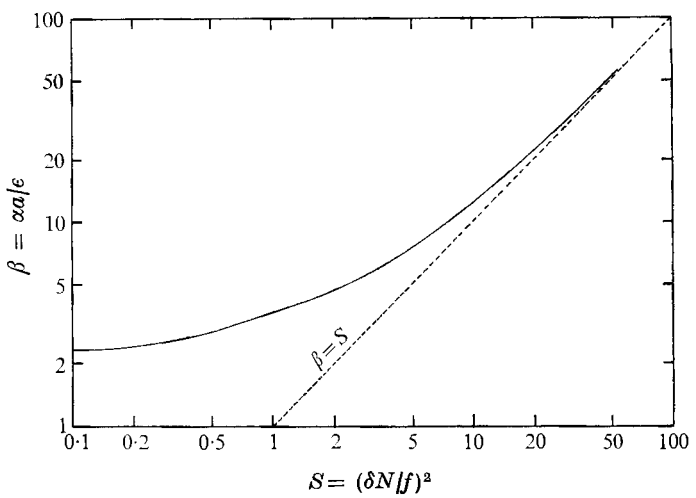

FIGURE 4. Plot of β required for a 'Taylor cone' to penetrate to the surface for a given S ($u_0'(z) = 0$).

We also observe that there is no critical magnitude for β: Taylor columns appear for all β, although they become more and more confined to the bottom as β decreases and may eventually be lost in the topography. It is interesting that the height of a column for $\beta < 2$ actually increases with stratification at small values of S. Finally we note that the explicit dependence on shear in this presentation is weak although there is an implicit dependence through $\beta = \alpha u_0(0)/\epsilon$.

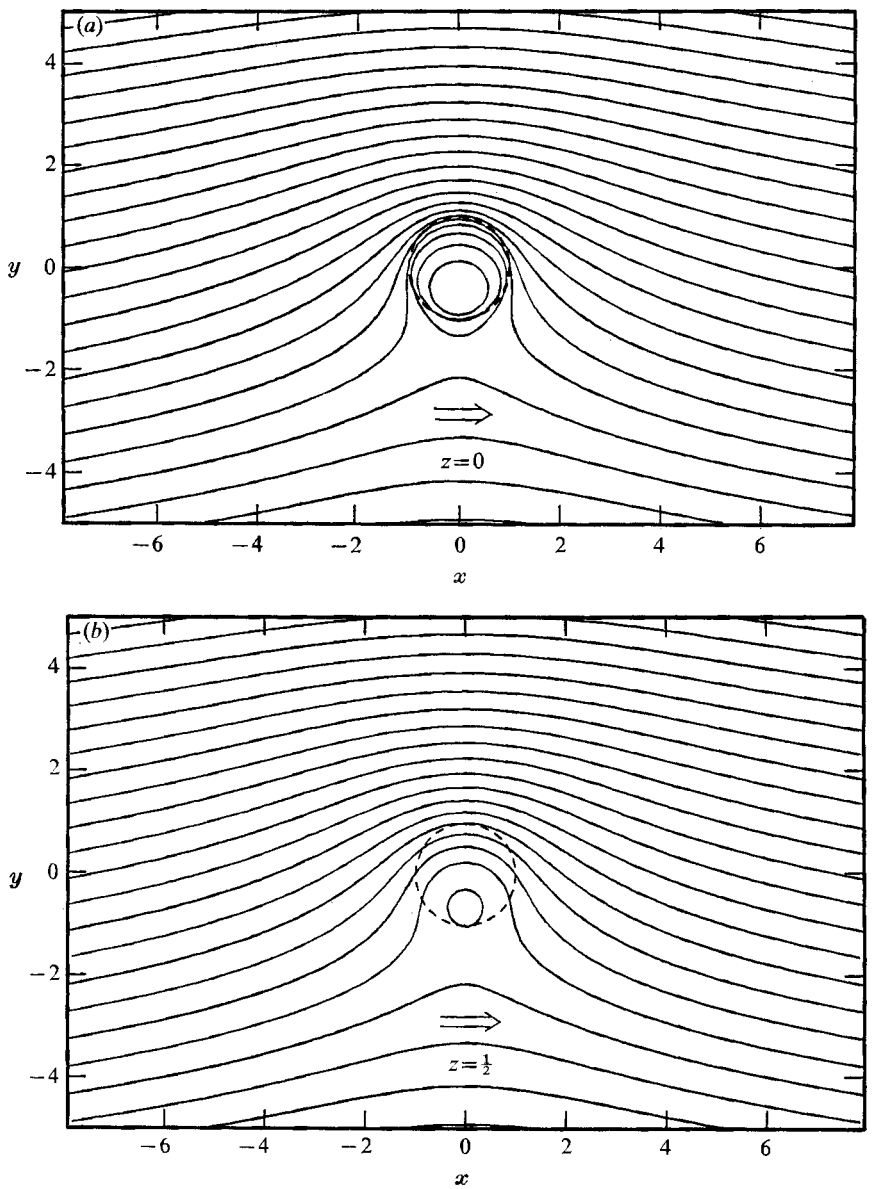

FIGURES 5(*a*, *b*). For legend see page 530.

Figure 4 gives the required β for a column to penetrate to the surface for a given S. Curves for the three values of $u_0'(z)$ are practically identical and approach the line $\beta = S$ for large S and the value $\beta = 2$ for small S.

In figure 5 we have drawn streamlines at the three levels $z = 0$, $z = \frac{1}{2}$ and $z = 1$ for $u_0'(z) = 1$, $\beta = 3$ and $S = 1$. The column, as outlined by the closed streamlines, is an anticyclonic vortex (a 'Taylor cone') sitting over the right-hand edge of the obstacle. From figure 3 its penetration height is about $z = 0{\cdot}6$, but observe that, even at the surface, a strong streamline distortion is felt.

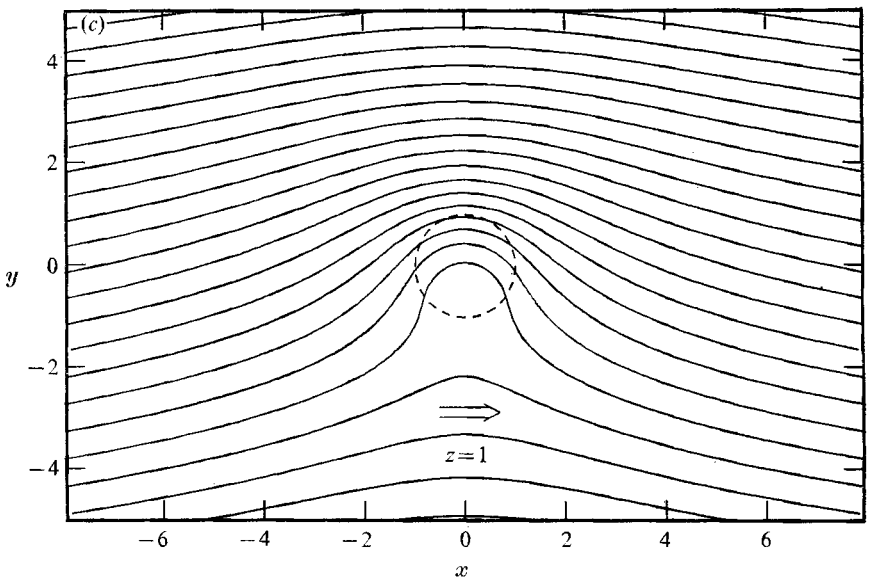

FIGURE 5. Streamline plot for $u_0'(z) = 1$, $\beta = 3$ and $S = 1$ at (*a*) $z = 0$, (*b*) $z = \frac{1}{2}$ and (*c*) $z = 1$. The obstacle is represented by the dashed circle of unit radius. Contours are lines of constant $p^{(0)}/u_0(z)$ obtained from (5·12).

6. Experimental verification

Davies (1971, 1972) has performed a series of experiments which were intended to explore the problems considered in the previous two sections. A cylindrical container 30 cm deep and 60 cm in diameter was filled while rotating with a stably stratified salt solution designed to give a linear density gradient. After waiting for the interior to be in solid-body rotation a small sphere of diameter 3·8 cm was set in motion horizontally in the azimuthal direction. Basing the Rossby number on the sphere radius and the Ekman number on the fluid depth Davies's flow had $\epsilon = 8{\cdot}8 \times 10^{-3}$ and $E = 7{\cdot}1 \times 10^{-6}$, so that $\epsilon > E^{\frac{1}{2}} = 2{\cdot}7 \times 10^{-3}$.

Qualitatively the flow observed by Davies is similar to that predicted. When the stratification is slight there is little attenuation of the obstacle disturbance with height but the attenuation increases with stratification. The lateral asymmetry of figure 5 is also seen but, as well, there is an upstream–downstream asymmetry reminiscent of the pattern predicted and observed by Vaziri & Boyer (1971) for homogeneous flow. Presumably this is a result of the fact that $\epsilon \approx 3E^{\frac{1}{2}}$ and vertical velocities induced through Ekman suction are not entirely negligible. The topographically forced negative vorticity induces a downward velocity in the Ekman layer over the obstacle which counteracts the vortex-line compression on the forward part of the obstacle and complements it on the rear.

Davies attempted to quantify the vertical influence of the obstacle by observing the horizontal distortion of radial dye lines at various levels. This distortion generally decreased in an exponential fashion with height allowing him to define an influence height as being the *e*-folding height on his fitted curves.

We could solve our problem for a hemispherical obstacle on a flat plane to

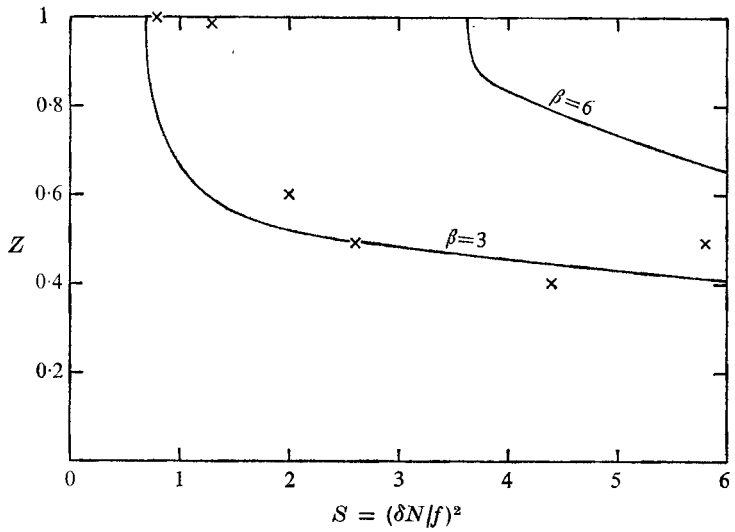

FIGURE 6. Comparison of the theoretical dependence of column height on stratification when $u_0'(z) = 0$ with experimental points of Davies (1971).

make it a closer approximation to the experiment. However, because of the difficulty in relating our methods of defining the Taylor column and the other approximations involved the effort would be pointless. Ingersoll (1969) found that the critical topographic parameter in the homogeneous problem with a hemisphere was increased from $\beta = 2$ to $3(\frac{3}{2})^{\frac{1}{2}}$. We relate the two problems by replacing Davies's sphere with a cylinder of effective height $1{\cdot}9(\frac{3}{2})^{-\frac{3}{2}}$ cm and placing it on a flat plane in a container of depth 19 cm (Davies's sphere was 19 cm below the upper surface). In this way we find that $\alpha = h_0/H = 0{\cdot}054$, giving $\beta = \alpha/\epsilon = 6$. In the experiment $u_0'(z) = 1$, so that $u_0(0) = 1$.

Davies used the ratio N/f as a measure of the stratification and was able to vary this from 0 to 0·24. Our $S = (\delta N/f)^2$ and therefore changes from 0 to 5·8. In figure 6 are shown Davies's measured column heights for those stratifications in which the column top, as defined by him, was within the container. We observe that the column height decreases rapidly at small S and then levels off to an almost constant value. The theoretical curve for $\beta = 6$ is shown but we find that the curve $\beta = 3$ gives much closer agreement.

Several explanations can be given for this discrepancy. Most important, Davies has used a different method for measuring column height and made his measurements after the Ekman layer at the bottom of the column had been allowed to perform its spin-up role. We would prefer to have column height measurements during the intermediate time between the time needed to actually establish the column and the spin-up time. More will be said on this point in § 7.

7. The inviscid limit

There are, at least, two difficulties associated with the application of analyses based on a vanishingly small viscosity.

Such a limit implies a large Reynolds number and indicates that flow separation from the obstacle will occur. In non-rotating situations at large Reynolds number fluid particles, within the viscous boundary layer near the obstacle, cannot follow highly curved paths in the lee (such as those illustrated in figure 5) because of the adverse pressure gradient associated with the regions of accelerated and decelerated flow. Instead the flow separates at the obstacle's lateral extreme and a smoother streamline pattern is established. In the rapidly rotating case, however, it appears that flow separation is inhibited until larger Reynolds numbers are reached. Perhaps this is because of the lowest order equivalence between the stream function and pressure: slowly moving particles in the boundary layer experience, mainly, a *lateral* pressure gradient from the Coriolis forces. Experiments on the homogeneous Taylor column (Vaziri & Boyer 1971) give remarkably good agreement with theory and no evidence of flow separation for Reynolds numbers as large as 400, based on the obstacle length scale, or 50 based on its height.

Closed streamlines, as we have found for all β with $S = O(1)$ and above a critical value in the other parameter ranges, represent another problem in the inviscid limit. Within these closed streamlines the fluid is isolated from the upstream flow and acted upon by viscous stresses at the boundaries and gradually loses its upstream history.

Mathematically the difficulty arises in deriving flow equations like (5.5). Potential vorticity from (5.4) is conserved along streamlines, but to obtain (5.5) we evaluated the conserved quantity far upstream. Closed streamlines do not terminate upstream and therefore, strictly speaking, the flow along them does not necessarily obey (5.5). In fact, additional solutions satisfying the appropriate equations outside the column and arbitrary conditions inside can be found.

For the homogeneous problem Ingersoll (1969) was able to include the effects of a vanishingly small viscosity. Using an inductive argument based on the circulation theorem and the fact that vorticity must be of $O(1)$ everywhere he showed that the ultimate state of the column must be stagnant. With $O(1)$ vorticity the bounding streamline must also have no motion along it and these conditions allow a unique determination of the exterior flow.

The circulation theorem is complicated in our problem by the inclusion of stratification and we have not been able to derive a similar result. However, the applicability of such an argument, if available, to many geophysical flows is questionable. It relies on the flow being steady long enough for the Ekman layers on the bounding surfaces of the Taylor column to spin up the interior to a new steady state (which is stagnant for the homogeneous case). For both homogeneous and non-homogeneous flows this time scale is of $O(E^{-\frac{1}{2}}f^{-1})$ (see, for example, Walin 1969; Buzyna & Veronis 1971), a considerable length of time for the earth's atmosphere and oceans.

For a broad class of initial conditions in an initial-value problem (for instance if the $t = 0$ flow field is horizontally uniform) it can be shown that

$$\frac{d}{dt}\left(\zeta^{(0)} - \frac{\rho_z^{(0)}}{S}\right) = 0, \tag{7.1}$$

with $d/dt = \partial/\partial t + \epsilon \mathbf{u}^{(0)}.\nabla$, t being time scaled by f^{-1}. Equation (7.1) says that even during the transient stage in the flow potential vorticity is conserved along streamlines. After the column has been established, on a time scale of the order of the advective time over the obstacle, fluid that becomes isolated will remember its upstream past and, at least until dissipation is felt (time scale $O(E^{-\frac{1}{2}}f^{-1})$), be governed by dynamics based on the upstream condition. A similar time-dependent form of the boundary conditions (5.7) and (5.8) can be derived.

We feel, therefore, that the results derived for $S \sim 1$ may be valid when applied to flow that can be considered steady on the advective time scale but unsteady on the spin-up time scale.

8. Observational evidence

The most celebrated evidence suggesting the natural occurrence of a Taylor column is Jupiter's Great Red Spot – a quasi-stationary phenomenon in one of the zonal belts of Jupiter's atmosphere. Hide (1961) first advanced the Taylor column hypothesis to explain the spot as a manifestation of the influence of a topographic feature in the lower atmosphere. Since then this speculation has been subject of some controversy.

Stone & Baker (1968) offered a qualitative analysis to show that density stratification could inhibit Taylor column development. By considering a balance between vertical advection and heat diffusion they showed that a critical parameter

$$Z = \sigma S/E^{\frac{1}{2}} \ll 1 \tag{8.1}$$

for two-dimensional motion. Available data suggested that $Z \gg 1$ for Jupiter. In order to ignore horizontal advection of heat a further ratio

$$UH^2/\kappa L \ll 1. \tag{8.2}$$

Stone & Baker believed this to be true, estimating $UH^2/\kappa L \approx 10^{-1}$. Hide (1969) challenged their value of $\kappa = 10^{10}\,\mathrm{cm^2\,s^{-1}}$, suggesting that it was incredibly large. A lower value ($\kappa < 10^8\,\mathrm{cm^2\,s^{-1}}$) invalidates (8.2) and makes (8.1) inapplicable. In this case our model equating vertical and horizontal advection is more appropriate.

Stone & Baker developed a second criterion based on the idea that two-dimensional motion was not possible if the upstream current contained significant vertical shear. As Hide (1971) and this paper have shown that this hypothesis is incorrect: the streamline pattern is independent of depth in a steady baroclinic flow provided that the two parameters $S \sim \epsilon \ll 1$ and diffusive effects can be neglected.

For flow in the neighbourhood of the Red Spot $\epsilon \approx 0{\cdot}04$ (Ingersoll). The stratification of the atmosphere is unknown, but Ingersoll calculates that $S \approx 0{\cdot}03$ for an isothermal atmosphere. These values clearly satisfy the requirements of § 4 and, as we showed in § 5, even $S = O(1)$ is not inconsistent with the Taylor column hypothesis provided that the obstacle is high enough. For a more direct comparison with flow in the region of the Red Spot it would be necessary to take into

account latitudinal variations in the Coriolis parameter (the latitudinal 'β-effect').

The earth's atmosphere is a somewhat different situation chiefly because of the reduced horizontal scales for major topographic features. Typical values for mountain ranges give $\epsilon \approx 0{\cdot}2$ and $S \approx 1{\cdot}5$ (Ingersoll). Even if our small Rossby number analysis should apply to flow with a Rossby number so close to unity we would need $\alpha > 2\epsilon/u_0(0)$ in order to have closed-streamline formation at moderate heights. Such a large value of α will correspond to an obstacle height almost filling the Taylor column. In addition, smaller scale irregularities (e.g. individual mountains) in the larger scale features we are considering will have much larger Rossby numbers associated with them and complicate our simplified picture. Latitudinal variations in f are also important.

Oceanic flows generally have a lower Rossby number chiefly because of their lower typical speeds. For argument's sake let us suppose that $U = 10\,\mathrm{cm\,s^{-1}}$, $f = 10^{-4}\,\mathrm{s^{-1}}$, $N = 2 \times 10^{-3}\,\mathrm{s^{-1}}$, $L = 50\,\mathrm{km}$ and $H = 4\,\mathrm{km}$. These values give $\epsilon = 0{\cdot}02$ and $S = 2{\cdot}6$, which fall nicely within the moderate stratification category of § 5. Referring to figure 4 we find that a topographic parameter $\beta = 5$ is sufficient at $S = 2{\cdot}6$ for the column to penetrate to the surface. Translating this into an obstacle height we find that

$$h_0 = 5H\epsilon\, U/u_0^*(0)$$
$$= 400U/u_0^*(0)\,\mathrm{m}.$$

A barotropic upstream flow would imply that an obstacle 400 m high would force a Taylor column penetrating to the surface. Generally $u_0^*(0) < U$ and $h_0 > 400\,\mathrm{m}$ is needed. Seamounts of these dimensions are a rather common feature of the ocean's bottom topography.

The fact that no direct observations of Taylor columns have been made in the ocean might seem remarkable considering the small topography necessary. One might explain this absence as being a result of violations by the ocean of some of the assumptions made in the analysis. Time dependence, dissipation, and non-uniformities in the upstream flow could each prevent such a phenomenon. However, an alternative explanation is that conventional measurement techniques using moored current meters are not an ideal means of observing these topographic effects and only scattered observations with the more satisfactory neutrally buoyant floats have been reported. Few hydrographic station networks have been of small enough scale to delineate such features.

There are a few observations which conform to the flow patterns computed in § 5. Fuglister (1963) reports on the track of a neutrally buoyant float as it travelled in the vicinity of Kelvin Seamount. The float was deflected to the left and accelerated as it passed some 500 m above the local bottom. The trajectory is very similar to one of the upper streamlines in figure 5. Meincke (1971) decribes an anticyclonic vortex trapped above Great Meteor Seamount. Doming of the isopycnals decreased with height, and contained rotational speeds of 3–7 $\mathrm{cm\,s^{-1}}$ which are not inconsistent, in our terms of reference, with the residual speeds of 1–3 $\mathrm{cm\,s^{-1}}$ found away from the seamount. Meincke explains the feature as being the result of tidal mixing. Defant (1961, p. 469) describes what

he calls a cyclonic vortex above Altair Seamount. The given mass field, however, is consistent with an anticyclonic vortex whose rotational speed increases with depth. It is interesting that the axis of the vortex tilts to the right (looking downstream) with height as is true of the case illustrated in figure 5.

Additional circumstantial evidence relating to the flow pattern on the bottom can be found in the configuration of sediments near seamounts. The streamline patterns in figure 5 are strongly asymmetric giving flow acceleration (reduced deposition) on the left and flow stagnation (enhanced deposition) on the right looking downstream. One well-documented seamount is the Knauss Knoll situated on the continental rise of the Western North Atlantic Ocean near Hudson Canyon in the middle of the Western Boundary Undercurrent. Lowrie & Heezen (1967) attempt to explain a large drift of sediments on the upstream end of the knoll by stagnation in a conventional symmetric flow. The echograms presented by them show a strong right–left asymmetry with a region of large deposition directly to the right of the knoll. This pattern agrees well with our analysis and the foredrift could well be the upstream extension of this slow water region.† Finally, Johnson, Vogt & Schneider (1971) report on a large number of seamounts in the Northeastern Atlantic many of which are almost surrounded by horseshoe-shaped moats or channels in the sediments at their bases. These moats are all breached by sediments on one side of the associated seamount and conform, qualitatively at least, to our flow patterns. Unfortunately, correlated current measurements are not available.

The work of § 4 for $S \sim \epsilon$ appears to have some application to what is known as the 'preconditioning phase' of bottom water formation in the northwest Mediterranean Sea. Observations reported by Swallow & Caston (1973) are consistent with there being a two-dimensional Taylor column trapped over a bulge in the continental slope bathymetric contours (Hogg 1973). The reader is referred to these accounts for the details.

9. Summary

We have shown that small bottom topography can have a significant effect at all depths on the slow steady flow of a rotating stratified fluid between plane horizontal boundaries even though the upstream state is baroclinic. This vertical influence depends primarily on the stratification measure S, the topographic parameter β and, to a lesser extent, the upstream shear $u_0'(z)$ for small Rossby number flows.

Very weak stratification ($S \ll \epsilon \ll 1$) cannot support a vertical shear in the horizontal flow, which must be two-dimensional even in the presence of topography. As was shown by Ingersoll (1969) a Taylor column appears over the right-hand edge of a right circular cylindrical obstacle when $\beta > 2$.

Weak stratification ($S \sim \epsilon \ll 1$) can support baroclinic motions and, in particular, an upstream shear $u_0'(z) \neq 0$ but we have shown, in agreement with Hide (1971), that the effect of topography on the horizontal streamlines remains

† Similar qualitative agreement has been found for two seamounts, Anton Dohrn and Rosemary Bank, in the Rockall Trough (Roberts *et al.* 1973).

depth independent. A Taylor column then exists when $\beta > 2$ for a right circular cylindrical obstacle.

Moderate stratification ($S \sim 1$) eliminates the two-dimensional constraint. We have outlined the manner in which the Taylor column collapses into a three-dimensional 'Taylor cone' and computed the dependence of the cone's penetration height upon β, $u_0'(z)$ and S (figure 3). Of particular significance are the facts that a Taylor cone exists no matter how small the magnitude of β and that, at constant β, the cone height decreases more and more slowly as S becomes large. A comparison of this cone height dependence on S with Davies's (1971, 1972) experimental work is qualitatively good (figure 6).

More work is needed both in the laboratory and the field. Previously reported observations from the ocean are suggestive but not conclusive. More exhaustive experiments into the effects of shear are needed and more attention must be paid to viscous stresses. Measurements of column height versus time in the parameter range $\epsilon \gg E^{\frac{1}{2}}$ would be very helpful in illuminating this latter problem.

My interest in this topic was kindled by discussions with Andrew Ingersoll at the 1970 Summer Study Program in Geophysical Fluid Dynamics at the Woods Hole Oceanographic Institution. The analysis and computations were performed while I was recipient of a National Research Council of Canada postdoctorate fellowship at the National Institute of Oceanography. I thank the N.I.O. staff for their hospitality and assistance. I am especially grateful to Steven Thorpe and David Roberts for their help and advice. Comments from a referee and Michael McIntyre helped clarify the presentation.

REFERENCES

BUZYNA, C. & VERONIS, G. 1971 Spin-up of a stratified fluid: theory and experiment. *J. Fluid Mech.* **50**, 579–608.

DAVIES, P. A. 1971 Experiments on Taylor columns in rotating, stratified fluids. Ph.D. thesis, University of Newcastle-upon-Tyne.

DAVIES, P. A. 1972 Experiments on Taylor columns in rotating stratified fluids. *J. Fluid Mech.* **54**, 691–718.

DEFANT, A. 1961 *Physical Oceanography*, vol. 1. Pergamon.

EADY, F. T. 1949 Long waves and cyclone waves. *Tellus*, **1**, 33–52.

FUGLISTER, F. C. 1963 Gulf Stream '60. *Progress in Oceanography*, vol. 1 (ed. M. Sears), pp. 265–373. Pergamon.

GRADSHTEYN, I. S. & RYZHIK, I. M. 1965 *Table of Integrals Series and Products*, 4th edn. Academic.

HIDE, R. 1961 Origin of Jupiter's Great Red Spot. *Nature*, **190**, 895–896.

HIDE, R. 1963 On the hydrodynamics of Jupiter's atmosphere. *Mem. Soc. Roy. Sci. Liège*, V **7**, 481–505.

HIDE, R. 1969 Dynamics of the atmospheres of the major planets with an appendix on the viscous boundary layer at the rigid bounding surface of an electrically-conducting rotating fluid in the presence of a magnetic field. *J. Atmos. Sci.* **26**, 841–853.

HIDE, R. 1971 On geostrophic motion of a non-homogeneous fluid. *J. Fluid Mech.* **49**, 745–751.

HIDE, R. & IBBETSON, A. 1966 An experimental study of 'Taylor columns'. *Icarus*, **5**, 279–290.

HIDE, R., IBBETSON, A. & LIGHTHILL, M. J. 1968 On slow transverse flow past obstacles in a rapidly rotating fluid, *J. Fluid Mech.* **32**, 251–272.

HOGG, N. G. 1973 The preconditioning phase of MEDOC 1969–II. Topographic effects. *Deep Sea Res.* (in press).

INGERSOLL, A. P. 1969 Inertial Taylor columns and Jupiter's Great Red Spot. *J. Atmos. Sci.* **26**, 744–752.

JACOBS, S. J. 1964 The Taylor column problem. *J. Fluid Mech.* **20**, 581–591.

JOHNSON, G. L., VOGT, P. R. & SCHNEIDER, E. D. 1971 Morphology of the Northeastern Atlantic and Labrador Sea. *Deut. Hydrograph. Z.* **24**, 49–73.

LOWRIE, A. & HEEZEN, B. C. 1967 Knoll and sediment drift near Hudson Canyon. *Science*, **157**, 1552–1553.

MEINCKE, J. 1971 Observation of an anticyclonic vortex trapped above a seamount. *J. Geophys. Res.* **76**, 7432–7440.

PROUDMAN, J. 1916 On the motion of solids in a liquid possessing vorticity. *Proc. Roy. Soc.* A **92**, 408–424.

ROBERTS, D. G., HOGG, N. G., BISHOP, D. G. & FLEWELLEN, C. G. **1973** Sediment distribution around moated seamounts in the Rockall Trough. (To appear.)

STONE, P. H. & BAKER, D. J. 1968 Concerning the existence of Taylor columns in atmospheres. *Quart. J. Roy. Met. Soc.* **94**, 576–580.

SWALLOW, J. C. & CASTON, G. F. 1973 The preconditioning phase of MEDOC 1969–I. Observations. *Deep Sea Res.* (in press).

TAYLOR, G. I. 1917 Motion of solids in fluids when the flow is not irrotational. *Proc. Roy. Soc.* A **93**, 99–113.

TAYLOR, G. I. 1923 Experiments on the motion of solid bodies in rotating fluids. *Proc. Roy. Soc.* A **104**, 213–218.

VAZIRI, A. & BOYER, D. L. 1971 Rotating flow over shallow topographies. *J. Fluid Mech.* **50**, 79–95.

WALIN, G. 1969 Some aspects of time-dependent motion of a stratified rotating fluid. *J. Fluid Mech.* **36**, 289–307.